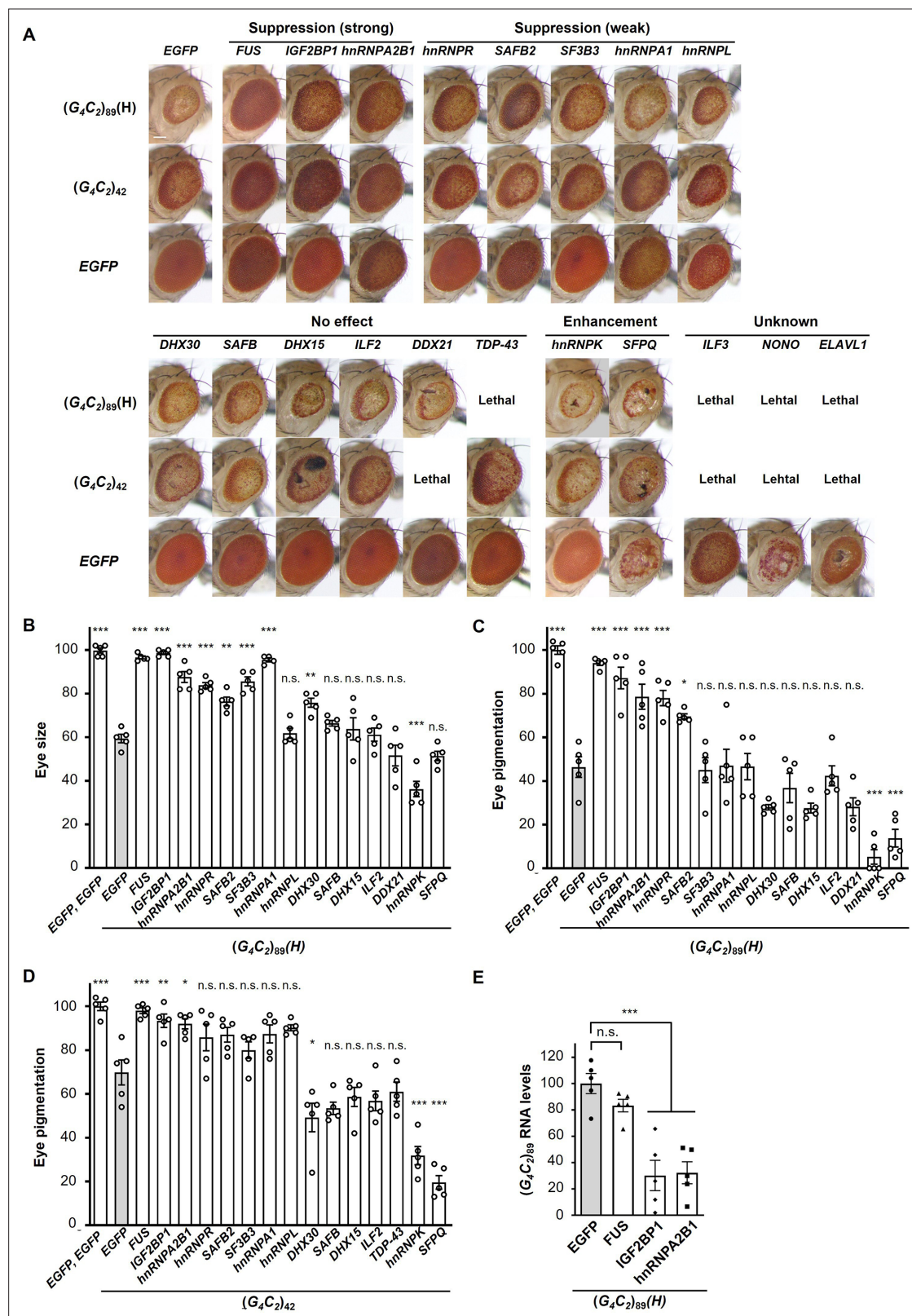


---

## Figures and figure supplements

FUS regulates RAN translation through modulating the G-quadruplex structure of GGGGCC repeat RNA in *C9orf72*-linked ALS/FTD

**Yuzo Fujino et al.**

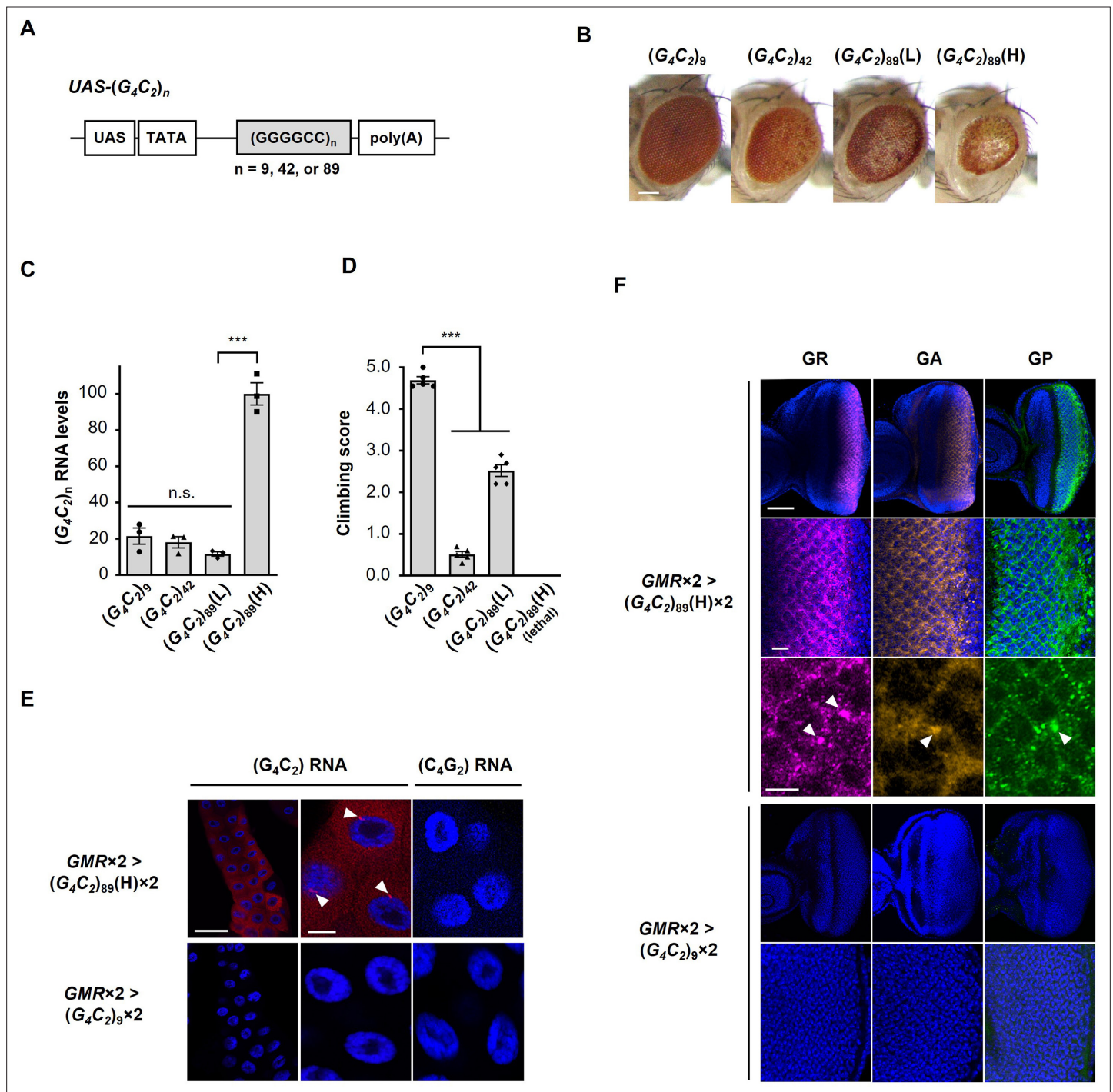


**Figure 1.** Screening for RNA-binding proteins (RBPs) that suppress G<sub>4</sub>C<sub>2</sub> repeat-induced toxicity in C9-ALS/FTD flies. **(A)** Light microscopic images of the eyes in flies expressing both (G<sub>4</sub>C<sub>2</sub>)<sub>42</sub> or <sub>89</sub> and the indicated RBPs using the GMR-Gal4 driver. Coexpression of FUS, IGF2BP1, or hnRNA2B1 suppressed eye degeneration in both (G<sub>4</sub>C<sub>2</sub>)<sub>42</sub> and (G<sub>4</sub>C<sub>2</sub>)<sub>89</sub> flies, indicated by ‘Suppression (strong).’ Coexpression of hnRNPR, SAFB2, SF3B3, hnRNPA1, or hnRNPL suppressed eye degeneration in either (G<sub>4</sub>C<sub>2</sub>)<sub>42</sub> or (G<sub>4</sub>C<sub>2</sub>)<sub>89</sub> flies, indicated by ‘Suppression (weak)’ (see also **Figure 1—source data 2**).

Figure 1 continued on next page

## Figure 1 continued

Scale bar: 100  $\mu$ m. **(B)** Quantification of eye size in  $(G_4C_2)_{89}$  flies coexpressing the indicated RBPs ( $n = 5$ ). **(C, D)** Quantification of eye pigmentation in  $(G_4C_2)_{89}$  flies **(C)** or  $(G_4C_2)_{42}$  flies **(D)** coexpressing the indicated RBPs ( $n = 5$ ). **(E)** Expression levels of  $(G_4C_2)_{89}$  RNA in flies expressing both  $(G_4C_2)_{89}$  and the indicated RBPs using the *GMR-Gal4* driver (five independent experiments,  $n = 25$  flies per genotype). The  $(G_4C_2)_{89}(H)$  fly line expresses  $(G_4C_2)_{89}$  RNA at a high level (see also **Figure 1—figure supplement 1**). In **(B–E)**, data are presented as the mean  $\pm$  SEM;  $p < 0.0001$ , as assessed by one-way ANOVA; n.s., not significant, \* $p < 0.05$ , \*\* $p < 0.01$ , and \*\*\* $p < 0.001$ , as assessed by Tukey's post hoc analysis. The detailed statistical information is summarized in **Figure 1—source data 3**.



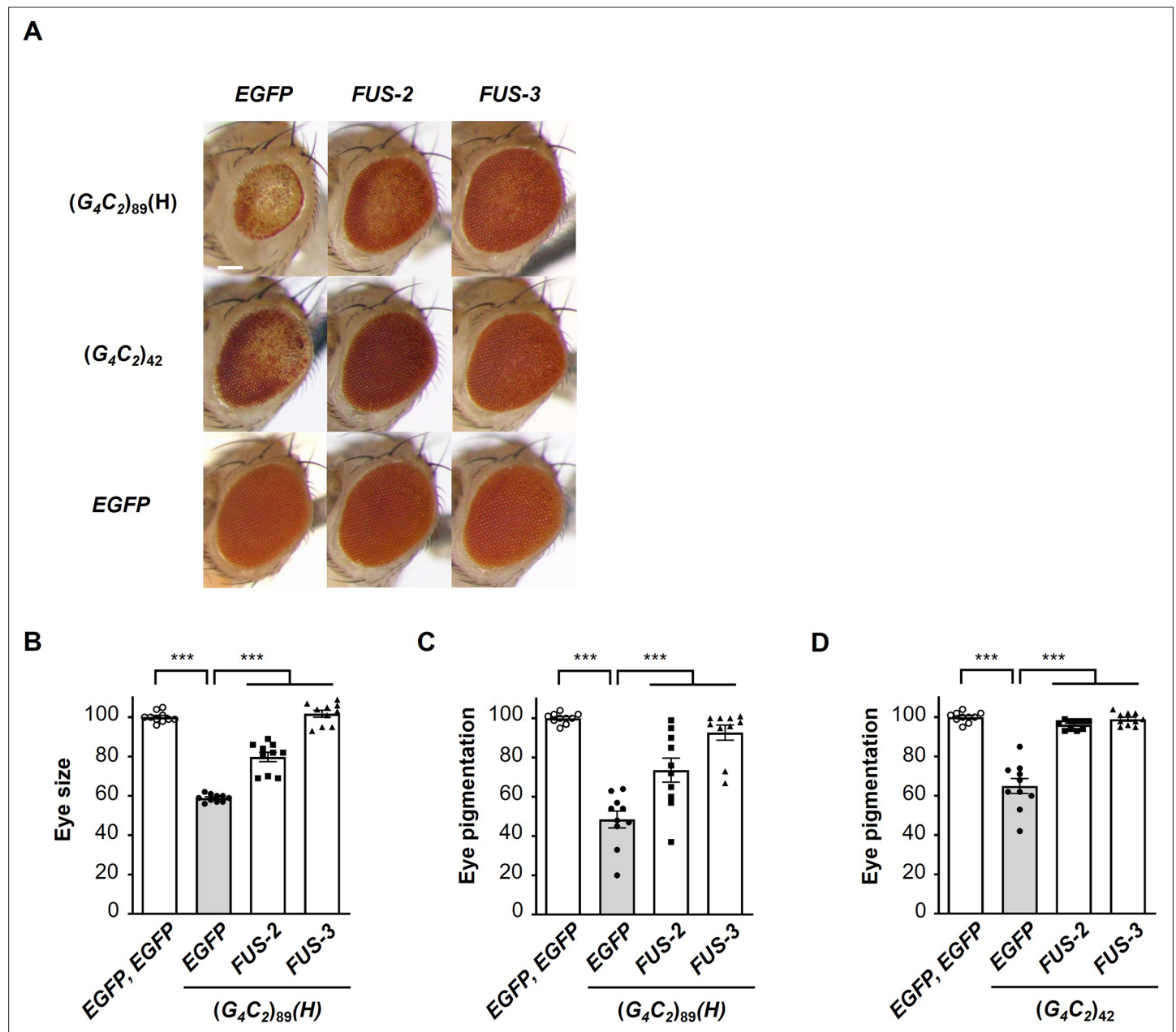
**Figure 1—figure supplement 1.** Characterization of C9-ALS/FTD flies. **(A)** (G<sub>4</sub>C<sub>2</sub>)<sub>n</sub> constructs used in this study. These constructs do not include an ATG start codon downstream of the UAS sequence, and were expressed in a tissue-specific manner using the GAL4-UAS system. **(B)** Light microscopic images of the eyes in flies expressing (G<sub>4</sub>C<sub>2</sub>)<sub>n</sub> using the GMR-Gal4 driver. Scale bar: 100 μm. **(C)** Expression levels of (G<sub>4</sub>C<sub>2</sub>)<sub>n</sub> RNAs in flies expressing (G<sub>4</sub>C<sub>2</sub>)<sub>n</sub> using the GMR-Gal4 driver. Strong eye degeneration with decreased eye size and loss of pigmentation was observed in (G<sub>4</sub>C<sub>2</sub>)<sub>42</sub> or <sub>89</sub> flies, but not in (G<sub>4</sub>C<sub>2</sub>)<sub>9</sub> flies. Eye degeneration was confirmed in (G<sub>4</sub>C<sub>2</sub>)<sub>42</sub> and two (G<sub>4</sub>C<sub>2</sub>)<sub>89</sub> independent fly lines. Degree of eye degeneration in two (G<sub>4</sub>C<sub>2</sub>)<sub>89</sub> fly lines was expression-level dependent [(L) vs. (H) in (G<sub>4</sub>C<sub>2</sub>)<sub>89</sub>] (three independent experiments, n = 15 flies per each genotype). Expression of G<sub>4</sub>C<sub>2</sub> repeat RNA of the sense transcripts but not that of the antisense transcripts was confirmed. **(D)** Climbing ability at 1 d of age in flies expressing (G<sub>4</sub>C<sub>2</sub>)<sub>n</sub> using the elav-Gal4 driver. Flies expressing (G<sub>4</sub>C<sub>2</sub>)<sub>89</sub>(H) in neurons showed lethality. Decreasing climbing ability was observed in (G<sub>4</sub>C<sub>2</sub>)<sub>42</sub> or <sub>89</sub> flies compared with (G<sub>4</sub>C<sub>2</sub>)<sub>9</sub> flies (five independent experiments, n = 100 flies per each genotype). **(E)** Fluorescence in situ hybridization (FISH) analyses of G<sub>4</sub>C<sub>2</sub> repeat RNA in the salivary glands of fly larvae with two copies of GMR-Gal4 and (G<sub>4</sub>C<sub>2</sub>)<sub>9</sub> or <sub>89</sub> (red: G<sub>4</sub>C<sub>2</sub> RNA; yellow: G<sub>2</sub>C<sub>4</sub> RNA; blue [DAPI]: nuclei). RNA foci formation

Figure 1—figure supplement 1 continued on next page

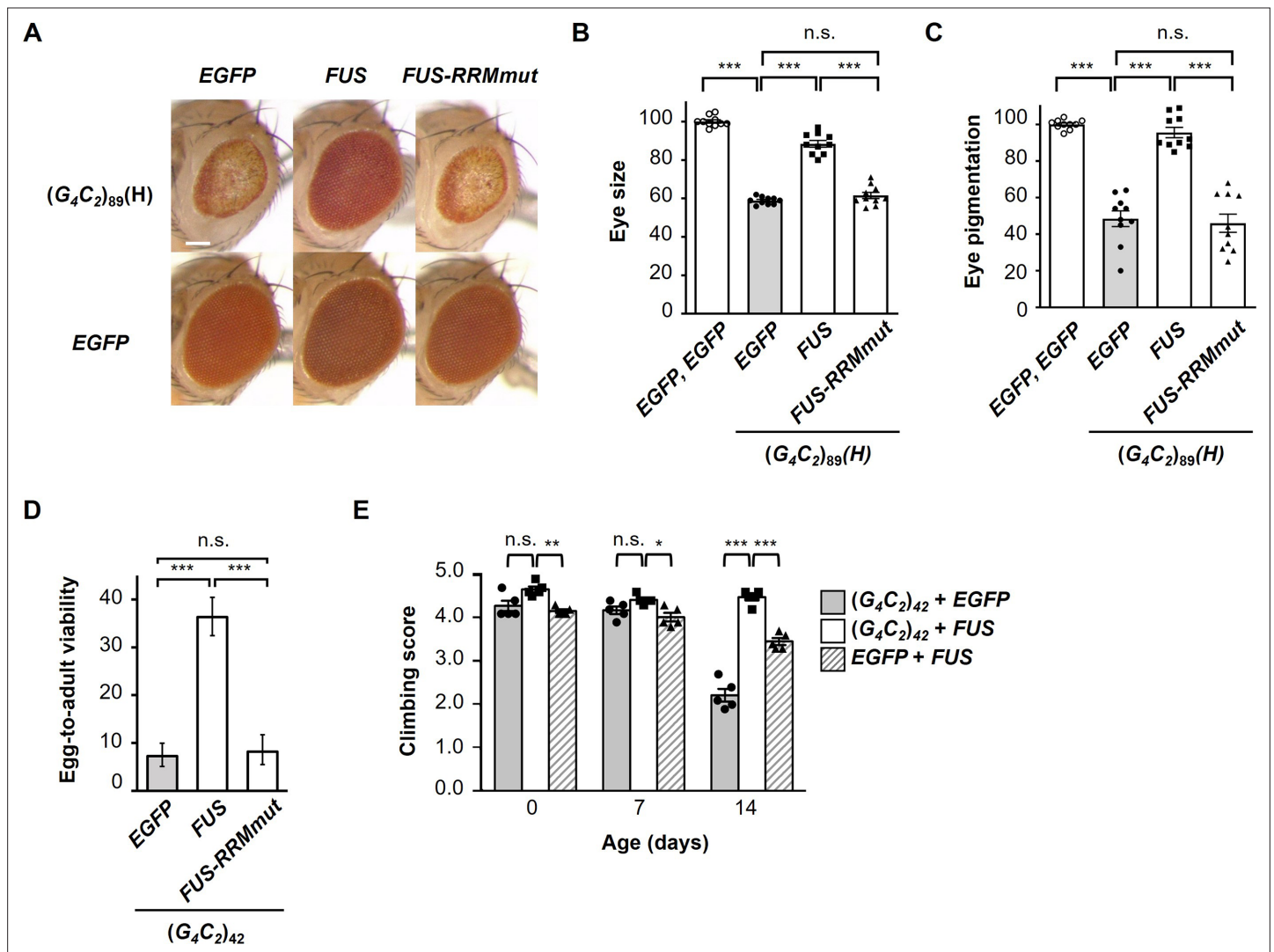


*Figure 1—figure supplement 1 continued*

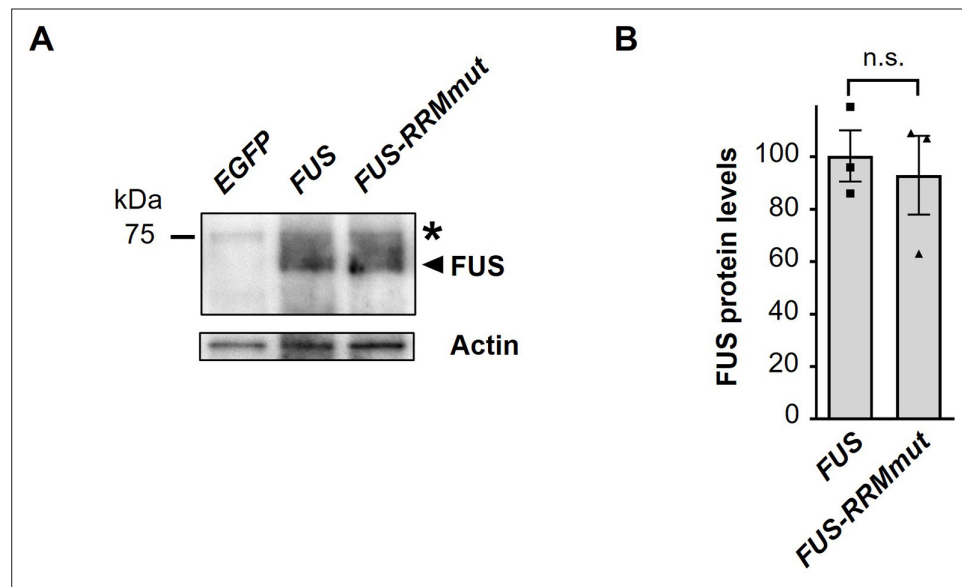
(arrowheads) of the sense transcripts but not that of the antisense transcripts was confirmed. RNA foci were observed in  $(G_4C_2)_{89}$  flies, but not in  $(G_4C_2)_9$  flies. Scale bars: 100  $\mu\text{m}$  (low magnification) or 20  $\mu\text{m}$  (high magnification). **(F)** Immunohistochemical analyses of dipeptide repeat proteins (DPRs) stained with anti-DPR antibodies in the eye imaginal discs of fly larvae with two copies of *GMR-Gal4* and  $(G_4C_2)_9$  or  $89$  (magenta: poly(GR); orange: poly(GA); green: poly(GP); blue [DAPI]: nuclei). Expression and cytoplasmic aggregation (arrowheads) of three DPRs in  $(G_4C_2)_{89}$  flies, but not in  $(G_4C_2)_9$  flies, were confirmed. Scale bars: 50  $\mu\text{m}$  (low magnification), 10  $\mu\text{m}$  (middle magnification), and 5  $\mu\text{m}$  (high magnification). In **(B–F)**, L: low-expression line; H: high-expression line. In **(C, D)**, data are presented as the mean  $\pm$  SEM;  $p < 0.0001$ , as assessed by one-way ANOVA; n.s., not significant, and \*\*\* $p < 0.001$ , as assessed by Tukey's post hoc analysis. The detailed statistical information is summarized in **Figure 1—figure supplement 1—source data 2**.



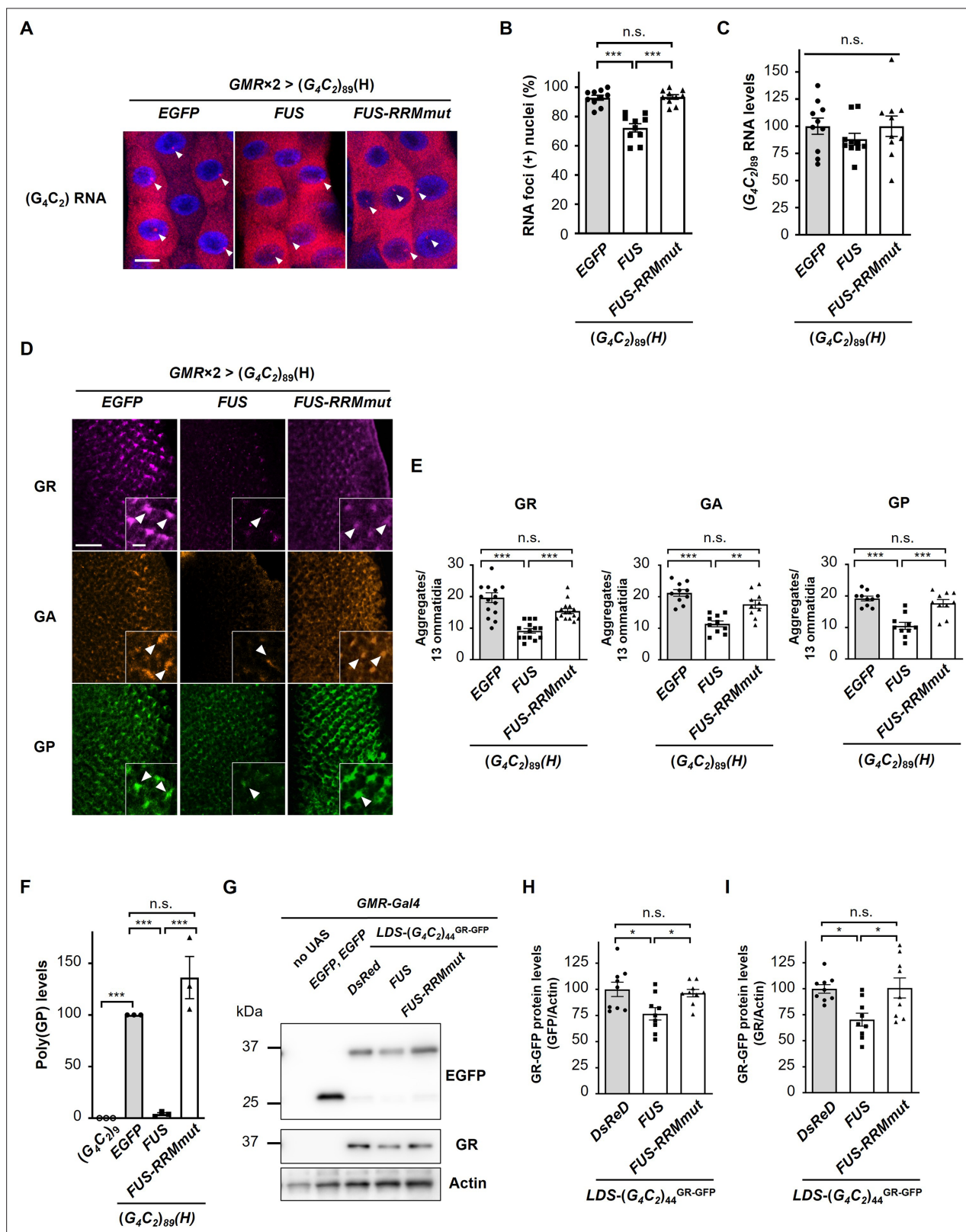
**Figure 1—figure supplement 2.** Coexpression of FUS suppresses  $G_4C_2$  repeat-induced toxicity in flies expressing  $(G_4C_2)_{89}$ . **(A)** Light microscopic images of the eyes in flies expressing both  $(G_4C_2)_{42}$  or  $89$  and FUS using the *GMR-Gal4* driver. FUS-2 and FUS-3 are different strains from that in **Figure 1**. Scale bar: 100  $\mu$ m. **(B)** Quantification of the eye size in  $(G_4C_2)_{89}$  flies of the indicated genotypes ( $n = 10$ ). **(C, D)** Quantification of eye pigmentation in  $(G_4C_2)_{89}$  flies **(C)** or  $(G_4C_2)_{42}$  flies **(D)** of the indicated genotypes ( $n = 10$ ). In **(B–D)**, data are presented as the mean  $\pm$  SEM;  $p < 0.0001$ , as assessed by one-way ANOVA; \*\*\* $p < 0.001$ , as assessed by Tukey's post hoc analysis. The detailed statistical information is summarized in **Figure 1—figure supplement 2—source data 1**.



**Figure 2.** FUS suppresses G<sub>4</sub>C<sub>2</sub> repeat-induced toxicity via its RNA-binding activity. **(A)** Light microscopic images of the eyes in flies expressing both (G<sub>4</sub>C<sub>2</sub>)<sub>89</sub> and either FUS or FUS-RRMmut using the GMR-Gal4 driver. Scale bar: 100  $\mu$ m. **(B)** Quantification of eye size in the flies of the indicated genotypes (n = 10). **(C)** Quantification of eye pigmentation in the flies of the indicated genotypes (n = 10). **(D)** Egg-to-adult viability in flies expressing both (G<sub>4</sub>C<sub>2</sub>)<sub>42</sub> and either FUS or FUS-RRMmut using the GMR-Gal4 driver (>500 flies per genotype). **(E)** Climbing ability in flies expressing both (G<sub>4</sub>C<sub>2</sub>)<sub>42</sub> and FUS using the elav-GeneSwitch driver (five independent experiments, n = 100 flies per each genotype). In **(B–E)**, data are presented as the mean  $\pm$  SEM. In **(B, C)**, p<0.0001, as assessed by one-way ANOVA; n.s., not significant, and \*\*\*p<0.001, as assessed by Tukey's post hoc analysis. In **(D)**, n.s., not significant and \*\*\*p<0.001, as assessed by Tukey's multiple-comparison test using wholly significant difference. In **(E)**, n.s., not significant, \*p<0.05, \*\*p<0.01, and \*\*\*p<0.001, as assessed by two-way repeated-measures ANOVA with Tukey's post hoc analysis. The detailed statistical information is summarized in **Figure 2—source data 1**.



**Figure 2—figure supplement 1.** Western blot analysis showing expression levels of FUS and FUS-RRMmut proteins. **(A)** Western blot analysis of the FUS and FUS-RRMmut proteins in the heads of adult flies expressing *EGFP*, *FUS*, or *FUS-RRMmut* using the *GMR-Gal4* driver, with an anti-FUS antibody. The arrowhead indicates bands from the FUS and FUS-RRMmut proteins, whereas the asterisk indicates bands resulting from nonspecific antibody binding. **(B)** Quantification of the FUS and FUS-RRMmut proteins from the western blot analysis in **(A)** ( $n = 3$ ). In **(B)**, data are presented as the mean  $\pm$  SEM; n.s., not significant, as assessed by the unpaired t-test. The detailed statistical information is summarized in **Figure 2—figure supplement 1—source data 1**.



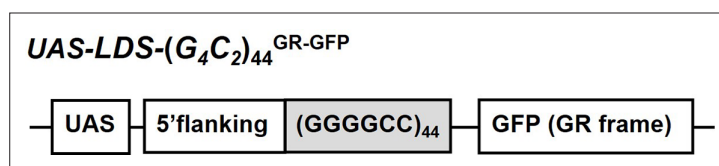
**Figure 3.** FUS suppresses RNA foci formation and RAN translation from G<sub>4</sub>C<sub>2</sub> repeat RNA. **(A)** Fluorescence in situ hybridization (FISH) analyses of G<sub>4</sub>C<sub>2</sub> repeat RNA in the salivary glands of fly larvae expressing both (G<sub>4</sub>C<sub>2</sub>)<sub>89</sub> and either FUS or FUS-RRMmut using two copies of the GMR-Gal4 driver (red: G<sub>4</sub>C<sub>2</sub> RNA; blue [DAPI]: nuclei). Arrowheads indicate RNA foci. Scale bar: 20  $\mu$ m. **(B)** Quantification of the number of nuclei containing RNA foci from the FISH analyses in **(A)** (n = 10). **(C)** Expression levels of (G<sub>4</sub>C<sub>2</sub>)<sub>89</sub> RNA in fly larvae expressing both (G<sub>4</sub>C<sub>2</sub>)<sub>89</sub> and either FUS or FUS-RRMmut using

Figure 3 continued on next page

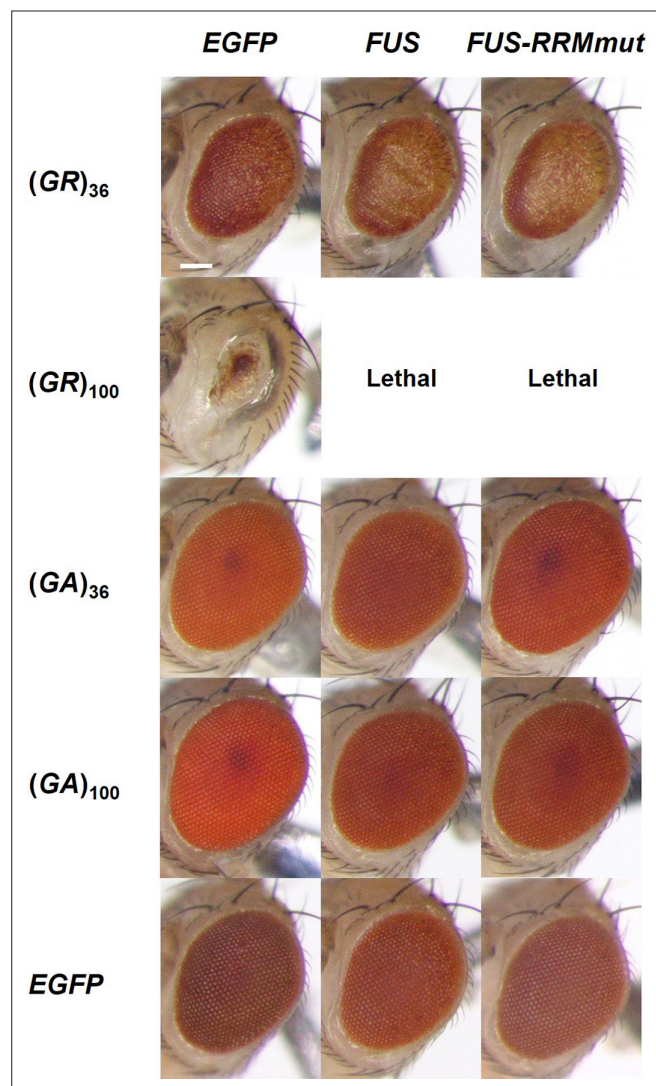


## Figure 3 continued

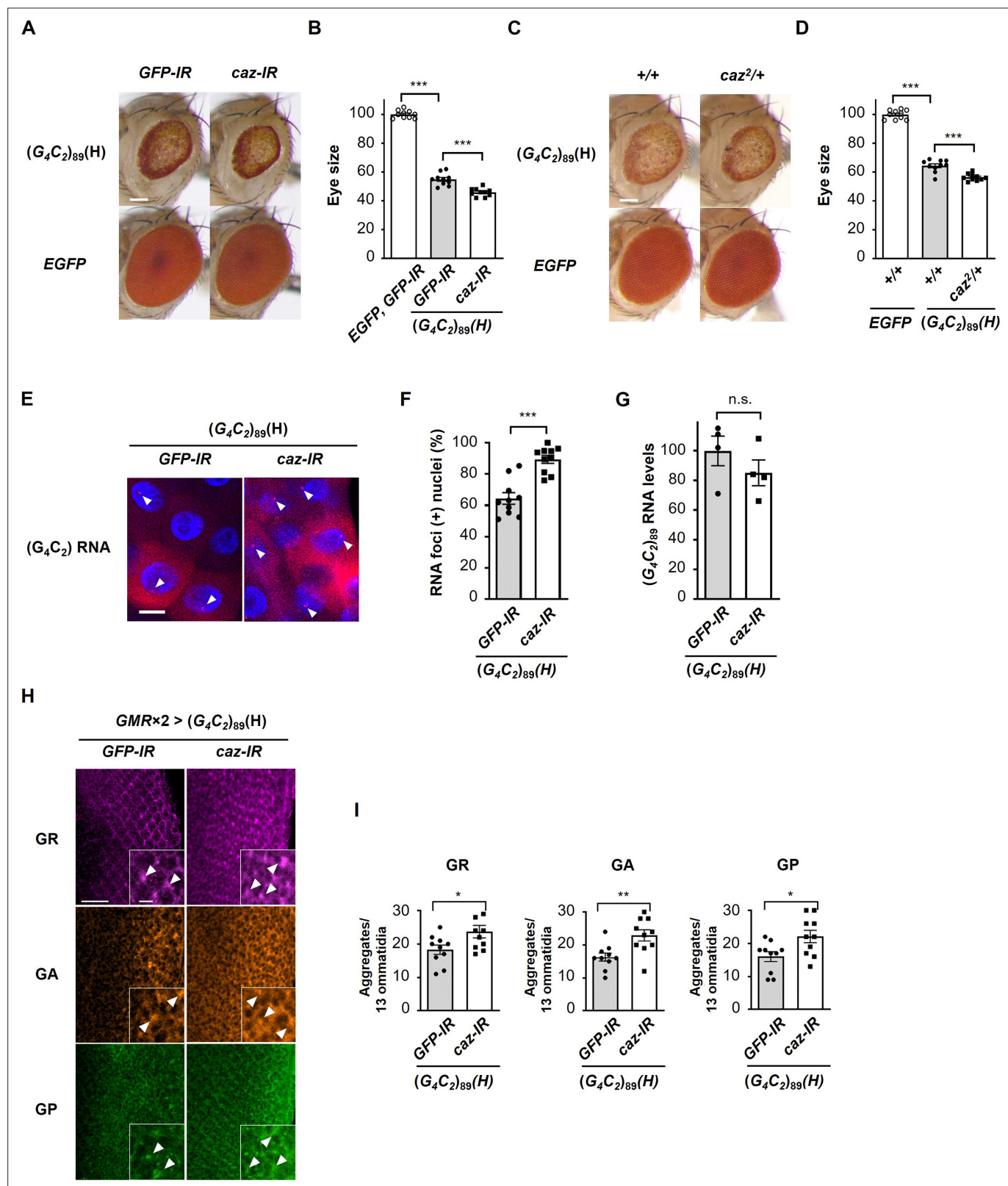
the *GMR-Gal4* driver (10 independent experiments,  $n = 50$  flies per each genotype). **(D)** Immunohistochemical analyses of dipeptide repeat proteins (DPRs) stained with anti-DPR antibodies in the eye imaginal discs of fly larvae expressing both  $(G_4C_2)_{89}$  and either *FUS* or *FUS-RRMmut* using two copies of the *GMR-Gal4* driver (magenta: poly(GR); orange: poly(GA); green: poly(GP)). Arrowheads indicate cytoplasmic aggregates. Scale bars:  $20\ \mu\text{m}$  (low magnification) or  $5\ \mu\text{m}$  (high magnification). **(E)** Quantification of the number of DPR aggregates from the immunohistochemical analyses in **(D)** ( $n = 14$  or  $15$  [GR], or  $10$  [GA or GP]). **(F)** Immunoassay to determine poly(GP) levels in flies expressing both  $(G_4C_2)_{89}$  and either *FUS* or *FUS-RRMmut* using the *GMR-Gal4* driver (three independent experiments,  $n = 30$  flies per each genotype). **(G)** Western blot analysis of the heads of adult flies expressing both  $\text{LDS-}(G_4C_2)_{44}^{\text{GR-GFP}}$  and any of *DsRed*, *FUS* or *FUS-RRMmut* using the *GMR-Gal4* driver, using either an anti-GFP (upper panel) or anti-GR antibody (middle panel). **(H, I)** Quantification of GR-GFP protein levels from the western blot analysis in **(G)** (nine independent experiments,  $n = 90$  flies per each genotype). In **(B, C, E, F, H, I)**, data are presented as the mean  $\pm$  SEM. In **(B, E, F)**,  $p < 0.0001$ , as assessed by one-way ANOVA; n.s., not significant, \* $p < 0.05$ , \*\* $p < 0.01$ , and \*\*\* $p < 0.001$ , as assessed by Tukey's post hoc analysis. In **(C)**,  $p = 0.452$ , as assessed by one-way ANOVA; n.s., not significant, as assessed by Tukey's post hoc analysis. In **(H)**,  $p = 0.0148$ , as assessed by one-way ANOVA; n.s., not significant and \* $p < 0.05$ , as assessed by Tukey's post hoc analysis. In **(I)**,  $p = 0.0072$ , as assessed by one-way ANOVA; n.s., not significant and \* $p < 0.05$ , as assessed by Tukey's post hoc analysis. The detailed statistical information is summarized in **Figure 3—source data 1**.



**Figure 3—figure supplement 1.** Schema of the *LDS-(G<sub>4</sub>C<sub>2</sub>)<sub>44</sub><sup>GR-GFP</sup>* construct. Schema of the *LDS-(G<sub>4</sub>C<sub>2</sub>)<sub>44</sub><sup>GR-GFP</sup>* construct containing the (G<sub>4</sub>C<sub>2</sub>)<sub>44</sub> sequence and 114 nucleotides of the 5'-flanking region of intron 1 of the human *C9orf72* G<sub>4</sub>C<sub>2</sub> repeat sequence. A GFP tag in the GR frame was introduced downstream of the (G<sub>4</sub>C<sub>2</sub>)<sub>44</sub> repeat sequence.



**Figure 3—figure supplement 2.** Overexpression of *FUS* does not suppress eye degeneration in dipeptide repeat protein (DPR)-only flies expressing DPRs translated from non-G<sub>4</sub>C<sub>2</sub> RNAs. Light microscopic images of the eyes in DPR-only flies coexpressing either the poly(GR) or poly(GA) protein, and either *FUS* or *FUS-RRMmut* using the *GMR-Gal4* driver. Overexpression of *FUS* did not suppress the eye degeneration in flies expressing either (GR)<sub>36</sub> or (GR)<sub>100</sub>. Overexpression of *FUS* also caused mild eye degeneration in flies expressing EGFP, (GA)<sub>36</sub>, or (GA)<sub>100</sub>, likely due to *FUS* toxicity.



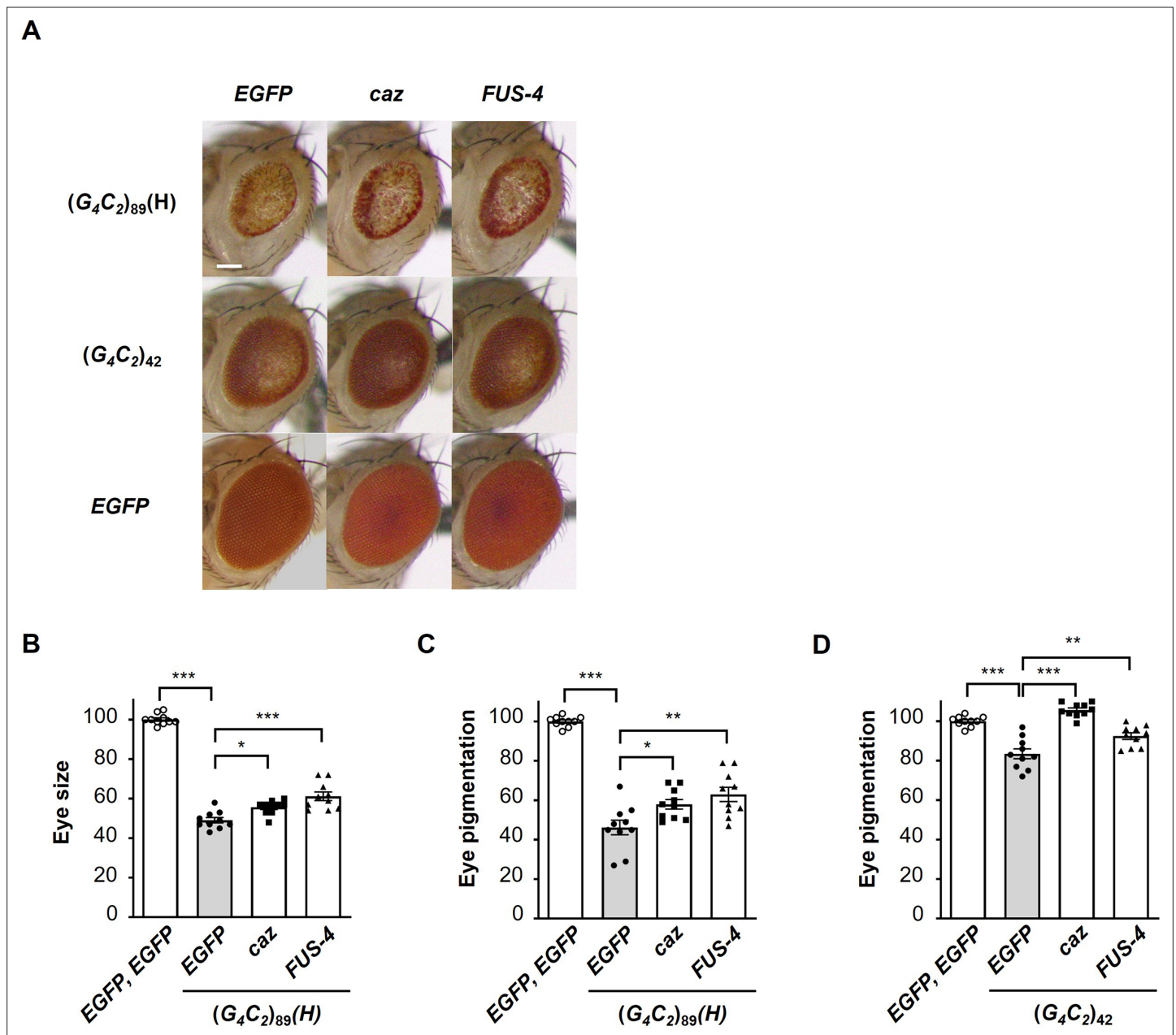
**Figure 4.** Reduction of endogenous *caz* expression enhances  $G_4C_2$  repeat-induced toxicity, RNA foci formation, and dipeptide repeat protein (DPR) aggregation. (A) Light microscopic images of the eyes in flies expressing  $(G_4C_2)_{89}$  using the *GMR-Gal4* driver, with knockdown of *caz*. Scale bar: 100  $\mu$ m. (B) Quantification of eye size in flies of the indicated genotypes shown in (A) ( $n = 10$ ). (C) Light microscopic images of the eyes in flies expressing  $(G_4C_2)_{89}$  using the *GMR-Gal4* driver, with a hemizygous deletion of *caz*. Scale bar: 100  $\mu$ m. (D) Quantification of eye size in the flies of the indicated genotypes.

Figure 4 continued on next page

## Figure 4 continued

shown in (C) (n = 10). (E) Fluorescence in situ hybridization (FISH) analyses of  $G_4C_2$  repeat RNA in the salivary glands of fly larvae expressing ( $G_4C_2$ )<sub>89</sub> using the *GMR-Gal4* driver, with knockdown of *caz* (red:  $G_4C_2$  RNA; blue [DAPI]: nuclei). Arrowheads indicate RNA foci. Scale bar: 20  $\mu$ m. (F) Quantification of the number of nuclei containing RNA foci from the FISH analyses in (E) (n = 10). (G) Expression levels of ( $G_4C_2$ )<sub>89</sub> RNA in fly larvae expressing ( $G_4C_2$ )<sub>89</sub> using the *GMR-Gal4* driver, with knockdown of *caz* (four independent experiments, n = 20 flies per each genotype). (H) Immunohistochemical analyses of DPRs stained with anti-DPR antibodies in the eye imaginal discs of fly larvae expressing ( $G_4C_2$ )<sub>89</sub> using two copies of the *GMR-Gal4* driver, with the knockdown of *caz*. (magenta: poly(GR); orange: poly(GA); green: poly(GP)). Arrowheads indicate cytoplasmic aggregates. Scale bars: 20  $\mu$ m (low magnification) or 5  $\mu$ m (high magnification). (I) Quantification of the number of DPR aggregates from the immunohistochemical analyses in (H) (n = 10). In (B, D, F, G, I), data are presented as the mean  $\pm$  SEM. In (B, D),  $p < 0.0001$ , as assessed by one-way ANOVA; \*\*\* $p < 0.001$ , as assessed by Tukey's post hoc analysis. In (F, G, I), n.s., not significant, \* $p < 0.05$ , \*\* $p < 0.01$ , and \*\*\* $p < 0.001$ , as assessed by the unpaired t-test. The detailed statistical information is summarized in **Figure 4—source data 1**.





**Figure 4—figure supplement 1.** Endogenous *caz* is a functional homologue of *FUS* for the suppression of  $G_4C_2$  repeat-induced toxicity. **(A)** Light microscopic images of the eyes in flies expressing both  $(G_4C_2)_{42}$  or  $89$  and either *caz* (FLAG-*caz*) or *FUS-4* (FLAG-*FUS*) using the *GMR-Gal4* driver. *FUS-4* is a different strain from those used in **Figure 1** and **Figure 1—figure supplement 2**. Scale bar: 100  $\mu$ m. **(B)** Quantification of the eye size in  $(G_4C_2)_{89}$  flies of the indicated genotypes ( $n = 10$ ). **(C, D)** Quantification of eye pigmentation in  $(G_4C_2)_{89}$  flies **(C)** or  $(G_4C_2)_{42}$  flies **(D)** of the indicated genotypes ( $n = 10$ ). In **(B–D)**, data are presented as the mean  $\pm$  SEM;  $p < 0.0001$ , as assessed by one-way ANOVA; n.s., not significant, \* $p < 0.05$ , \*\* $p < 0.01$ , and \*\*\* $p < 0.001$ , as assessed by Tukey's post hoc analysis. The detailed statistical information is summarized in **Figure 4—figure supplement 1—source data 1**.

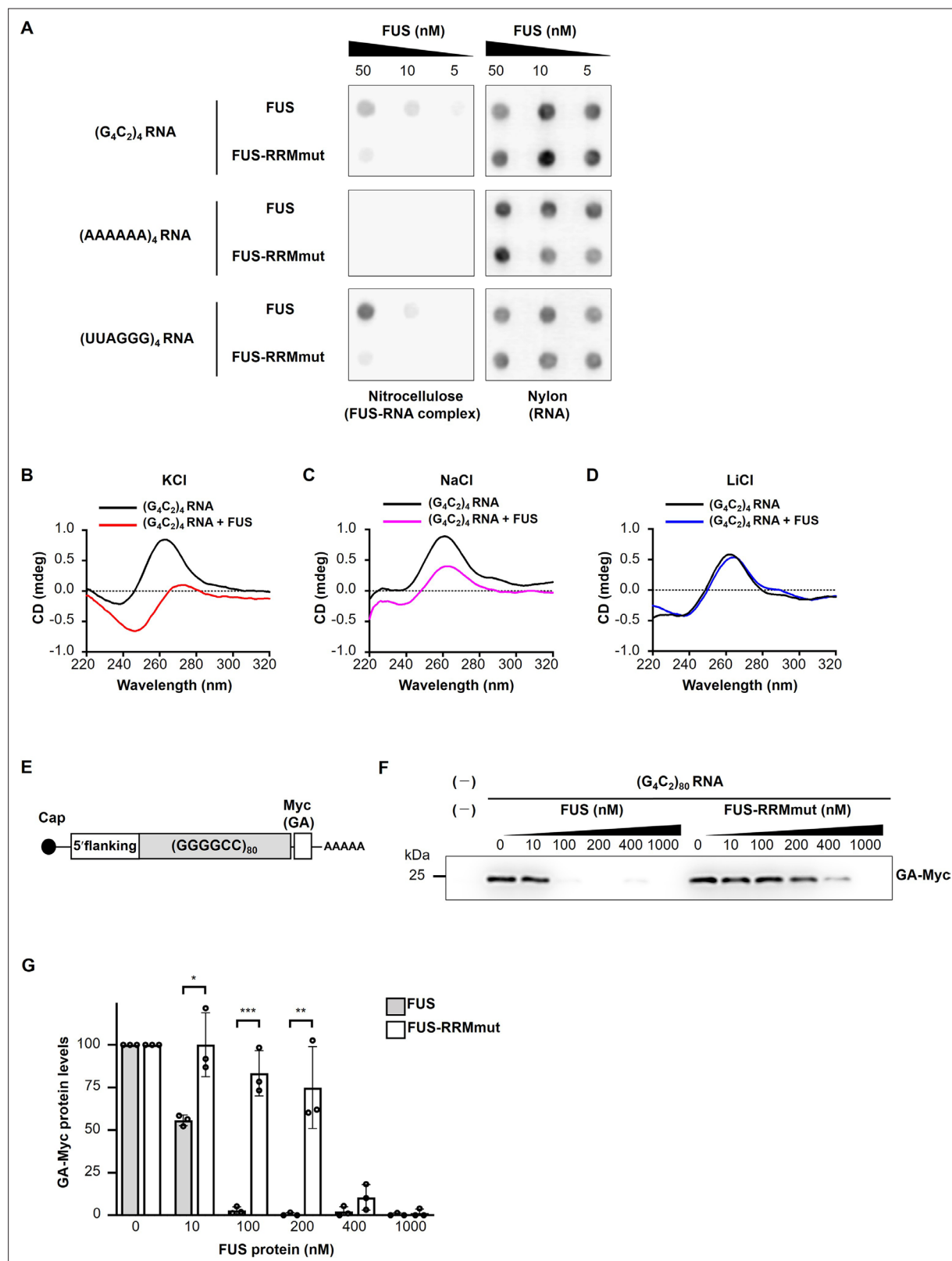


**Figure 5.** FUS directly binds to and modulates the G-quadruplex structure of  $G_4C_2$  repeat RNA, resulting in the suppression of RAN translation in vitro. **(A)** Analysis of the binding of His-tagged FUS proteins to biotinylated  $(G_4C_2)_4$  RNA by the filter binding assay. The nitrocellulose membrane (left) traps RNA-bound FUS proteins, whereas unbound RNAs are recovered on the nylon membrane (right), and then the RNAs trapped on each of the membranes was probed with streptavidin-horseradish peroxidase (HRP). Biotinylated  $(AAAAA)_4$  and  $(UUAGGG)_4$  were used as negative and positive

Figure 5 continued on next page

*Figure 5 continued*

controls, respectively. **(B–D)** CD spectra of  $(G_4C_2)_4$  RNA incubated with or without FUS in the presence of 150 mM KCl **(B)**, NaCl **(C)**, or LiCl **(D)**. The CD spectrum of FUS alone was subtracted from that of  $(G_4C_2)_4$  RNA incubated with FUS. The original data are shown in **Figure 5—figure supplement 2B–2D**. **(E)** Schema of the template RNA containing the  $(G_4C_2)_{80}$  sequence and 113 nucleotides of the 5'-flanking region of intron 1 of the human *C9orf72*  $G_4C_2$  repeat sequence. A Myc tag in the GA frame was introduced downstream of the  $(G_4C_2)_{80}$  repeat sequence. **(F)** Western blot analysis of samples from in vitro translation using rabbit reticulocyte lysate in the presence or absence of increasing concentrations of FUS or FUS-RRMmut. The GA-Myc fusion protein was detected by western blotting using the anti-Myc antibody. **(G)** Quantification of the GA-Myc fusion protein in **(F)** ( $n = 3$ ). In **(G)**, data are presented as the mean  $\pm$  SEM; \* $p < 0.05$ , \*\* $p < 0.01$ , and \*\*\* $p < 0.001$ , as assessed by the unpaired  $t$ -test. The detailed statistical information is summarized in **Figure 5—source data 1**.

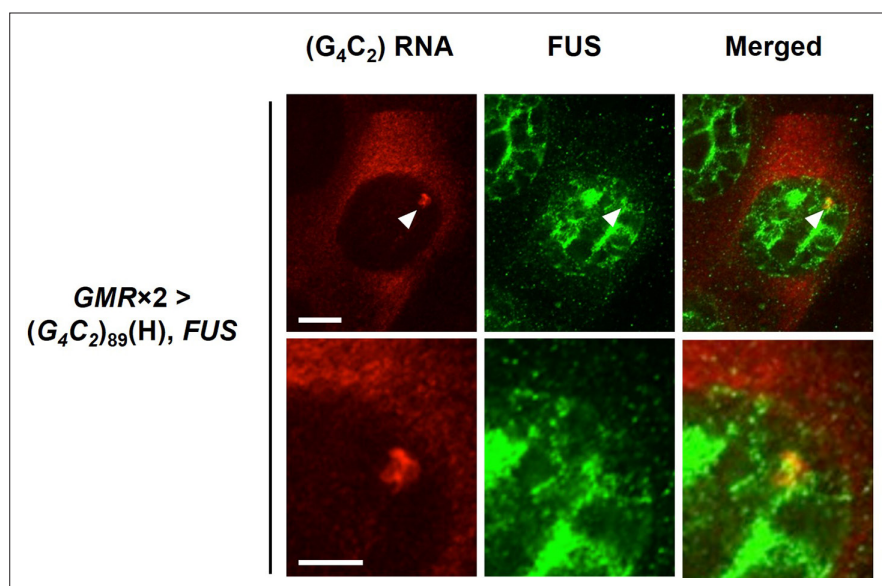


**Figure 5—figure supplement 1.** FUS colocalizes with  $G_4C_2$  RNA foci. Combined fluorescence in situ hybridization (FISH) and immunohistochemical analyses of  $G_4C_2$  repeat RNA and FUS in the salivary glands of flies expressing both  $(G_4C_2)_{89}$  and FUS using two copies of the *GMR-Gal4* driver. Arrowheads indicate colocalization of FUS with RNA foci. Scale bar: 10  $\mu$ m (low magnification) and 5  $\mu$ m (high magnification).

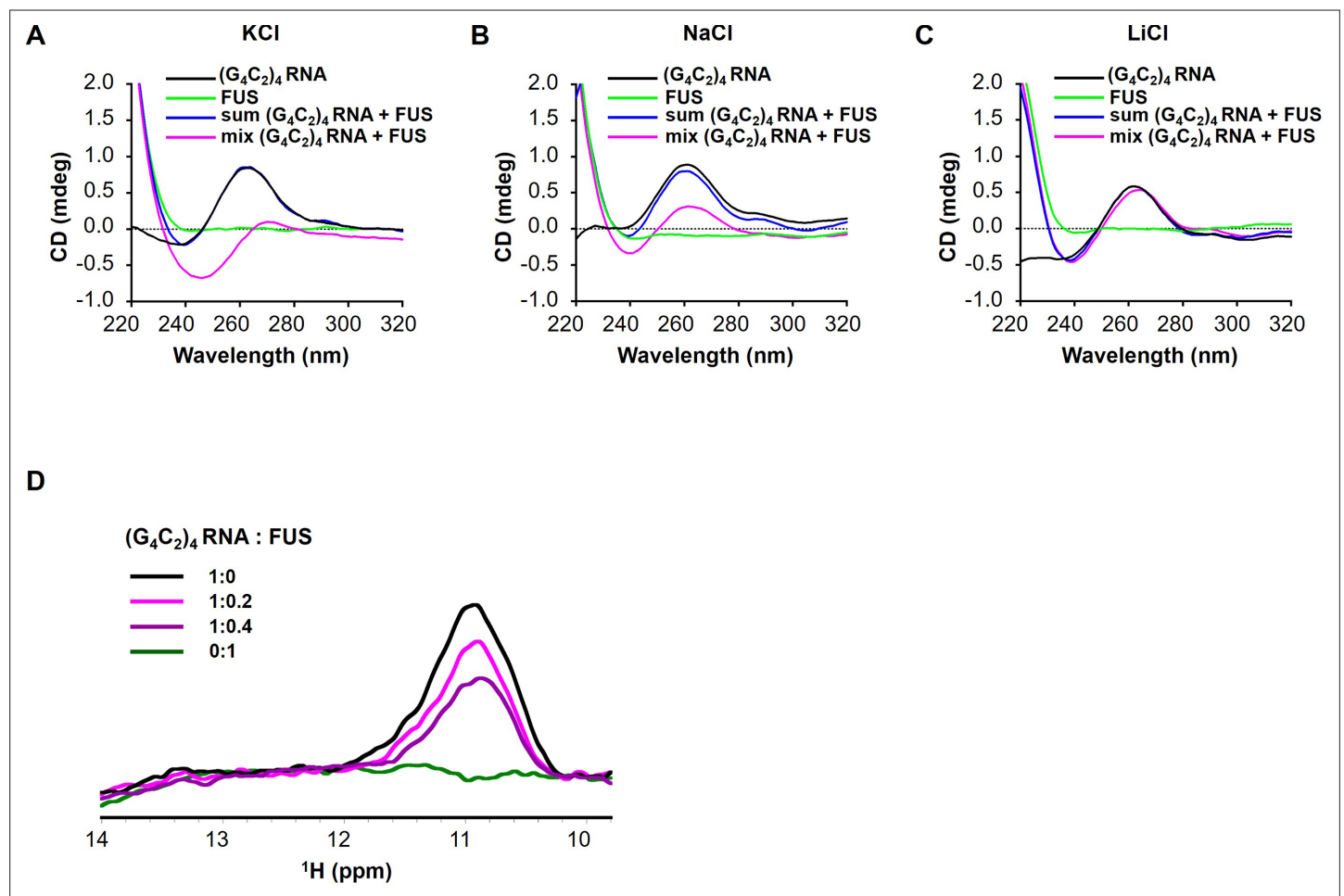


**Figure 5—figure supplement 2.** FUS modulates the G-quadruplex structure of  $G_4C_2$  repeat RNA. (A–C) CD spectra of  $(G_4C_2)_4$  RNA incubated with or without FUS in the presence of 150 mM KCl (A), NaCl (B), or LiCl (C). CD spectra of  $(G_4C_2)_4$  RNA alone (black), FUS alone (green), sum of  $(G_4C_2)_4$  RNA and FUS (blue), and the spectra of their coincubation (magenta) are shown. FUS interacts with  $(G_4C_2)_4$  RNA under KCl or NaCl buffer conditions. (D) Imino proton NMR spectra of  $(G_4C_2)_4$  RNA incubated with increasing amounts of FUS in the presence of 150 mM KCl.



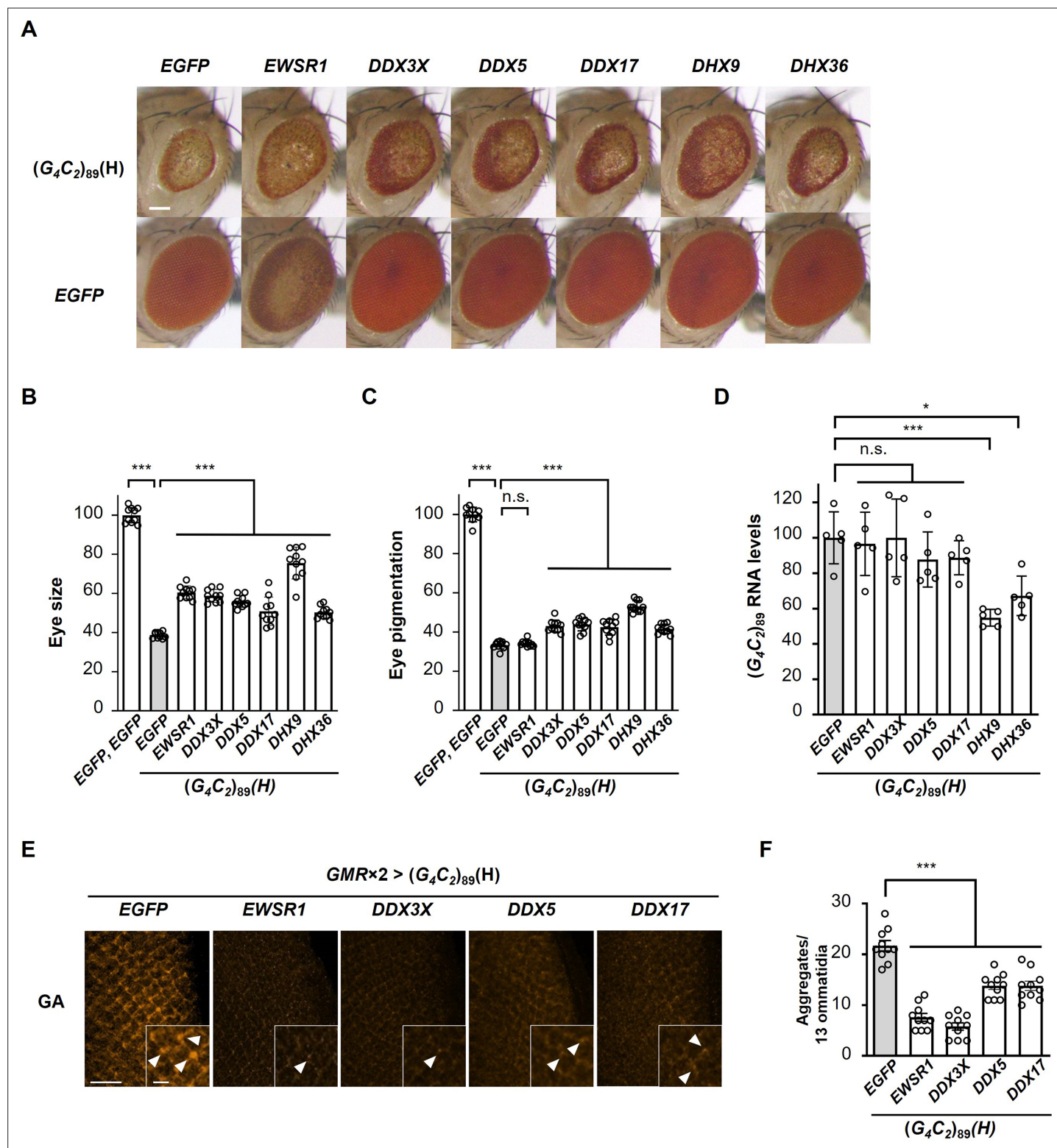


**Figure 6.** Identification of G-quadruplex-targeting RNA-binding proteins (RBPs) that suppress  $G_4C_2$  repeat-induced toxicity in C9-ALS/FTD flies. (A) Light microscopic images of eyes in flies expressing both  $(G_4C_2)_{89}$  and the indicated G-quadruplex-targeting RBPs using the *GMR-Gal4* driver. Scale bar: 100  $\mu$ m. (B) Quantification of eye size in the flies of the indicated genotypes ( $n = 10$ ). (C) Quantification of eye pigmentation in the flies of the indicated genotypes ( $n = 10$ ). (D) Expression levels of  $(G_4C_2)_{89}$  RNA in flies expressing both  $(G_4C_2)_{89}$  and the indicated G-quadruplex-targeting RBPs using the *GMR-Gal4* driver (five independent experiments,  $n = 25$  flies per each genotype). (E) Immunohistochemical analyses of poly(GA) stained with anti-GA antibody in the eye imaginal discs of fly larvae expressing both  $(G_4C_2)_{89}$  and the indicated G-quadruplex-targeting RBPs using two copies of the

Figure 6 continued on next page

*Figure 6 continued*

*GMR-Gal4* driver (orange: poly(GA)). Arrowheads indicate cytoplasmic aggregates. Scale bars: 20  $\mu\text{m}$  (low magnification) or 5  $\mu\text{m}$  (high magnification). (F) Quantification of the number of poly(GA) aggregates from the immunohistochemical analyses in (E) ( $n = 10$ ). In (B, C, D, F), data are presented as the mean  $\pm$  SEM;  $p < 0.0001$ , as assessed by one-way ANOVA; n.s., not significant, \* $p < 0.05$  and \*\*\* $p < 0.001$ , as assessed by Tukey's post hoc analysis. The detailed statistical information is summarized in **Figure 6—source data 2**.